Suppression of Lung Adenocarcinoma Progression by Nkx2-1

Monte M. Winslow[1,2], Talya L. Dayton[1], Roel G. W. Verhaak[5,6], Caroline Kim-Kiselak[1], Eric L. Snyder[1], David M. Feldser[1], Diana D. Hubbard[5,6], Michel J. DuPage[1], Charles A. Whittaker[1], Sebastian Hoersch[1], Stephanie Yoon[1], Denise Crowley[1], Roderick T. Bronson[7], Derek Y. Chiang[5,6,8], Matthew Meyerson[5,6], and Tyler Jacks[1,2,3,4,*]

[1]David H. Koch Institute for Integrative Cancer Research, [2]Ludwig Center for Molecular Oncology, [3]Department of Biology, [4]Howard Hughes Medical Institute, Massachusetts Institute of Technology, Cambridge, Massachusetts, USA, [5]Dana-Farber Cancer Institute, Harvard University, Cambridge, Massachusetts, USA, [6]Broad Institute, Cambridge, Massachusetts, USA, [7]Department of Biomedical Sciences, Tufts University Veterinary School, North Grafton, Massachusetts, USA, [8]Department of Genetics, University of North Carolina, North Carolina, USA.

Despite the high prevalence and poor outcome of patients with metastatic lung cancer, the mechanisms of tumour progression and metastasis remain largely uncharacterized. We modelled human lung adenocarcinoma, which frequently harbours activating point mutations in KRAS[1] and inactivation of the p53-pathway[2], using conditional alleles in mice[3-5]. Lentiviral-mediated somatic activation of oncogenic Kras and deletion of p53 in the lung epithelial cells of *Kras*$^{LSL\text{-}G12D/+}$;*p53*$^{flox/flox}$ mice initiates lung adenocarcinoma development[4]. Although tumours are initiated synchronously by defined genetic alterations, only a subset become malignant, suggesting that disease progression requires additional alterations. Identification of the lentiviral integration sites allowed us to distinguish metastatic from non-metastatic tumours and determine the gene expression

alterations that distinguish these tumour types. Cross-species analysis identified the NK-2 related homeobox transcription factor Nkx2-1 (Ttf-1/Titf1) as a candidate suppressor of malignant progression. In this mouse model, downregulation of Nkx2-1 is pathognomonic of high-grade poorly differentiated tumours. Gain- and loss-of-function experiments in cells derived from metastatic and non-metastatic tumours demonstrated that Nkx2-1 controls tumour differentiation and limits metastatic potential *in vivo*. Interrogation of Nkx2-1 regulated genes, analysis of tumours at defined developmental stages, and functional complementation experiments indicate that Nkx2-1 constrains tumours in part by repressing the embryonically-restricted chromatin regulator Hmga2. While focal amplification of *NKX2-1* in a fraction of human lung adenocarcinomas has focused attention on its oncogenic function[6-9], our data specifically link Nkx2-1 downregulation to loss of differentiation, enhanced tumour seeding ability, and increased metastatic proclivity. Thus, the oncogenic and suppressive functions of Nkx2-1 in the same tumour type substantiate its role as a dual function lineage factor.

We developed lentiviral vectors that express Cre-recombinase (Lenti-Cre)[10] and determined the dose that results in 5 to 20 lung tumours per $Kras^{LSL\text{-}G12D/+};p53^{flox/flox}$ mouse after intratracheal administration. Mice with this tumour multiplicity lived 8-14 months after tumour initiation and developed frequent macroscopic metastases to the draining lymph nodes, pleura, kidneys, heart, adrenal glands, and liver (Supplementary Fig. 1). Because lentiviruses integrate stably into the genome, the integration site was a unique molecular identifier that unambiguously linked primary tumours to their related metastases (Fig. 1a). We used linker-mediated PCR (LM-PCR) to determine the genomic sequence directly 3' of the integrated lentiviral genome followed by a specific PCR for the lentiviral integration site (Fig. 1b). To have samples of sufficient quantity and purity for our analyses, we derived cell lines from primary tumours and metastases.

Cell lines were composed of pure tumour cells as determined by complete recombination of the *p53*^{floxed} alleles (data not shown). The clonal relationship of these cell lines was established using LM-PCR or Southern blot analysis for the lentiviral genome (Fig. 1c and data not shown). We termed cell lines derived from verified metastatic primary lung tumours T_{Met}.

Gene expression profiling was performed on cell lines from twenty-three lung tumours and metastases (nine metastases, seven T_{Met} primary tumours, and seven potentially non-metastatic primary tumours). Using an unsupervised consensus clustering method[11], we identified four cell lines from likely non-metastatic tumour samples that had highly concordant gene expression and were separate from all T_{Met} and metastasis (Met) samples (Supplementary Fig. 2). Therefore, we surmised that these could represent non-metastatic primary tumours and classified them T_{nonMet}.

To determine whether relevant phenotypic differences existed between T_{nonMet} and T_{Met} cell lines, we assayed their ability to establish experimental metastases. T_{Met} cell lines consistently formed more tumour nodules in the liver after intrasplenic injection despite having equivalent proliferation rates in cell culture (Fig. 1d-e and Supplementary Fig. 2). The differences between T_{nonMet} and T_{Met} in metastatic potential, gene expression profiles, and our subsequent analyses suggest that T_{nonMet} cell lines likely originated from non-metastatic tumours.

Significant gene expression alterations distinguished T_{nonMet} from T_{Met} and Met-derived cell lines (Fig. 1f and Supplementary Table 1), many of which were validated by qRT-PCR, flow cytometry, and western blotting (data not shown). A gene expression signature generated by comparing T_{nonMet} to T_{Met}/Met samples predicted patient outcome in two human lung adenocarcinoma gene expression datasets[12,13], suggesting the possibility of evolutionarily-conserved molecular mechanisms of tumour progression

(Supplementary Fig. 2). Thus, we integrated mouse and human data by comparing the differences in expression between T_{nonMet} and T_{Met}/Met samples with the association of human gene expression and patient survival (Fig. 2a). Two genes were particularly notable from this analysis: the NK-related homeobox transcription factor *Nkx2-1* and the Nkx2-1 target gene surfactant protein B (*Sftpb*; Fig. 2a). Nkx2-1 regulates lung development and is expressed in Type II pneumocytes and bronchiolar cells in the adult[14-16]. Expression of *Nkx2-1* was >10-fold higher in T_{nonMet} samples, and higher *NKX2-1* expression in human tumours correlated with longer survival. Of note, *NKX2-1* is focally amplified in ~10% of human lung adenocarcinomas, with previous functional data supporting oncogenic activity[6-9]. Conversely some, but not all, immunohistochemical analyses of NKX2-1 in lung adenocarcinoma suggest an association between NKX2-1-negative tumours and poor patient outcome[17-19]. Given the uncertain functional role of Nkx2-1 in human lung cancer, we focused on validating and characterizing the function of this transcription factor in suppressing tumour progression and metastasis.

We confirmed reduced Nkx2-1 mRNA and protein in T_{Met} and Met cell lines without evidence of focal genomic loss of this region (Fig. 2b, Supplemental Fig. 4, and data not shown). Analysis of tumours from our mouse model indicated that Nkx2-1 expression was consistently downregulated in high-grade poorly differentiated tumours (Fig. 2c-e and Supplementary Fig. 3). Nkx2-1 expression was also reduced in advanced $Kras^{G12D}$-driven lung adenocarcinomas with $p53^{R270H}$ or $p53^{R172H}$ point mutations[4,20]. Using our LM-PCR assay, we identified three primary lung tumours as metastatic based on the presence of metastases with the same lentiviral integration site (Fig. 1b and data not shown). These tumours each contained poorly differentiated areas that were Nkx2-1^{neg} (Supplementary Fig. 6). Interestingly, Nkx2-1 expression was low/absent in almost all lymph node and distant macrometastases, though some micrometastases were Nkx2-1^{pos} or Nkx2-1^{mixed} (Supplementary Fig. 3). Whether certain micrometastases were seeded

by Nkx2-1^{pos} cells or reverted to an Nkx2-1^{pos} phenotype due to cues from their new environment is unknown.

In human lung adenocarcinoma[12,13] the expression of *NKX2-1* correlated with a T_{nonMet} gene expression signature derived from the mouse (T_{nonMet} Signature; Fig. 2f and Supplementary Fig. 3). Additionally, the T_{nonMet} signature was anti-correlated with an embryonic stem cell signature, supporting the notion that T_{Met}/Met cells have transitioned to a less differentiated and more stem-like state[21] (Fig. 2f and Supplementary Fig. 3).

The correlative mouse and human data were consistent with Nkx2-1 being either a marker or a functional regulator of tumour progression. To interrogate the function of Nkx2-1, we reexpressed Nkx2-1 in a T_{Met} cell line. Nkx2-1 reexpression greatly suppressed tumour formation after intravenous transplantation (Fig. 3a, 3b, Supplementary Fig. 5, and data not shown). Moreover, of the tumours that formed after injection of T_{Met}-*Nkx2-1* cells, many were either Nkx2-1^{neg} or Nkx2-1^{mixed} (Fig. 3c). In general, tumours that continued to express Nkx2-1 were well differentiated, while Nkx2-1^{neg} tumours often displayed solid architecture or areas of poorly-differentiated cells (Fig. 3d and Supplementary Fig. 5). Intrasplenic transplantation unveiled a similar diminution of tumour formation by T_{Met}–*Nkx2-1* cells (Supplementary Fig. 5). Nkx2-1 reexpression did not alter proliferation or cell death in cell culture or affect tumour proliferation *in vivo* suggesting that Nkx2-1 specifically alters tumour seeding capacity (Supplementary Fig.5 and data not shown). Consistent with this hypothesis, Nkx2-1 reexpression dramatically reduced the ability of these cells to grow in anchorage-independent conditions and T_{Met}–*Nkx2-1* cells initiated tumours less efficiently after subcutaneous transplantation (Fig. 3e and Supplementary Fig. 5)

To further elucidate the functional effect of Nkx2-1 expression, we used RNAi to knock down Nkx2-1 in T_{nonMet} cell lines. Expression of *shNkx2-1* in T_{nonMet} cells reduced Nkx2-1 mRNA and protein to levels similar to those in T_{Met} cell lines (Supplementary Fig. 7 and data not shown). *Nkx2-1* knockdown allowed the formation of more liver nodules after intrasplenic injection and more lung nodules after intravenous transplantation (Fig. 3f). Furthermore, T_{nonMet}-*shNkx2-1* cells metastasized from these lung nodules to the draining mediastinal lymph nodes (data not shown). Mechanistically, Nkx2-1 knockdown did not alter proliferation or cell death in cell culture (Supplementary Fig. 7). However, Nkx2-1 knockdown enhanced the ability of cells to form colonies under anchorage-independence conditions and tumours after subcutaneous transplantation (Fig 3g and Supplementary Fig. 7) both of which are associated with increased cellular stress. To confirm that the effects of the *shNkx2-1* were specifically due to Nkx2-1 knockdown, we reexpressed an *Nkx2-1* cDNA (*Nkx2-1**) containing four silent point mutations rendering it insensitive to our *shNkx2-1*. Expression of *Nkx2-1** reverted the phenotypic alterations elicited by *shNkx2-1* (Fig. 3h). As a final test of the ability of Nkx2-1 to constrain tumour progression, we induced tumours in $Kras^{LSL\text{-}G12D/+};p53^{flox/flox}$ mice with either Lenti-Cre or a lentiviral vector expressing both Nkx2-1 and Cre (Lenti-Nkx2-1/Cre). Expression of exogenous Nkx2-1 limited tumour progression resulting in fewer tumours of advanced histopathological grades (Fig. 3i).

To discover Nkx2-1 regulated genes, we compared gene expression in T_{nonMet} and T_{nonMet}–*shNkx2-1* cells. Overlapping this gene list with the list of genes that are expressed at different levels in T_{nonMet} versus T_{Met}/Met cells uncovered a number of high priority candidate genes (Supplementary Fig. 8). We elected to focus on Hmga2 given its role in altering global gene expression through the regulation of chromatin structure and its association with embryonic and adult stem cell states[22-25]. Several reports suggest that Hmga2 can also be expressed in malignant tumours of diverse origins[26-29].

Hmga2 is derepressed by Nkx2-1 knockdown in T_{nonMet} cells and regions of *Kras*$^{G12D/+}$;*p53*$^{\Delta/\Delta}$ tumours that lacked Nkx2-1 expression were almost universally Hmga2^{pos} (Fig. 4a-c). Importantly, Nkx2-1^{neg} areas of known metastatic primary tumours and of metastases were Hmga2^{pos} (Supplementary Fig. 9 and data not shown). Additionally, Hmga2 was downregulated in T_{Met} cells after reexpression of *Nkx2-1* cDNA and in T_{nonMet}-*shNkx2-1* cells after expression of Nkx2-1* (data not shown).

Although Hmga2 can be regulated by the Let7 family of miRNAs[22,26,30], Let7 levels, *Lin28* expression, and Let7 activity were equivalent in T_{nonMet}, T_{Met}, and Met cell lines and were unaltered in T_{nonMet}-*shNkx2-1* cells (Supplementary Fig. 10 and data not shown). *Hmga2* promoter activity was derepressed in T_{nonMet}-*shNkx2-1* cells and repressed in T_{Met}-*Nkx2-1* cells, indicating that expression of Hmga2 in lung adenocarcinoma cells is regulated through differential promoter activity (Supplementary Fig. 10).

We hypothesized that lung adenocarcinomas progress from an Nkx2-1^{pos}Hmga-2^{neg} to an Nkx2-1^{neg}Hmga-2^{pos} state. However, metastatic and non-metastatic tumours could be fundamentally distinct at the time of initiation. Hmga2 is highly expressed in embryonic lung but not in any normal adult lung cells, and early after initiation, *Kras*$^{G12D/+}$;*p53*$^{\Delta/\Delta}$ tumours were uniformly Nkx2-1^{pos}Hmga-2^{neg} (Fig. 4d, Supplementary Fig. 11 and data not shown). *Kras*$^{G12D/+}$;p53-proficient tumours, which maintain their differentiated phenotype and never metastasize even late after tumour initiation[5], were almost universally Nkx2-1^{pos}Hmga-2^{neg} (Fig. 4e and Supplementary Fig. 11). Finally, at later time points poorly differentiated areas of *Kras*$^{G12D/+}$;*p53*$^{\Delta/\Delta}$ tumours with reduced Nkx2-1 expression were almost always associated with lower grade Nkx2-1-expressing areas (Supplementary Fig. 6). Collectively, these data indicate that lung adenocarcinomas undergo a transition towards a more aggressive Nkx2-1^{neg}Hmga-2^{pos}

phenotype and that a Nkx2-1-dependent gene expression program is a key regulator of this transition.

We next analyzed the expression of NKX2-1 and HMGA2 in human adenocarcinomas. Although the expression patterns were diverse, two important conclusions could be made. First, tumours of the NKX2-1^{pos}HMGA2^{neg} and NKX2-1^{neg}HMGA2^{pos} phenotypes exist within the spectrum of human lung adenocarcinomas (Fig. 4f and Supplementary Fig. 10). Second, there was a trend towards well-differentiated tumours being NKX2-1^{pos}/HMGA2^{neg} whereas moderately and poorly differentiated tumours were more often represented by other combinations of these proteins. Most notably, the moderately and poorly differentiated groups contained NKX2-1^{neg}/HMGA-2^{pos} tumours (Fig. 4f). These results underscore the diversity within this single human tumour type and suggest that our genetically defined model likely represents, at the molecular level, a subset of these tumours.

We next used RNAi to knockdown *Hmga2* in T_{nonMet}-*shNkx2-1* cells to determine if this gene was required for their enhanced metastasis seeding potential. Hmga2 knockdown greatly reduced tumour formation after transplantation (Fig. 4g and Supplementary Fig. 12). Finally, Hmga2 knockdown in a metastasis-derived cell line reduced anchorage-independent growth and tumour seeding ability after transplantation (Fig 4h-i and Supplementary Fig. 12). Expression of HMGA2 correlates with poor outcome and the presence of metastases in several cancer types (Supplemental Fig. 9)[26-29]. A future challenge will be to understand the molecular mechanism by which Hmga2 controls lung adenocarcinoma metastatic potential. The expansion of Nkx2-1^{neg}Hmga-2^{pos} regions within primary lung tumours suggests the acquisition of phenotypes that are advantageous to the primary tumours and also increase the probability of metastatic spread.

The fact that NKX2-1 can have both oncogenic and tumour suppressive functions in lung cancer presumably represents dichotomous functions within the distinct context of individual tumours of the same type. Lung adenocarcinomas may be diverse in their cell of origin, mutation spectrum, or gene expression leading to a differential requirement for continued NKX2-1 expression and different ability to tolerate or benefit from NKX2-1 downregulation. Our results emphasize the power of genetically-engineered mouse models of advanced disease, used in conjunction with human studies, to elucidate mechanisms that control cancer progression and metastatic spread. Through this approach we identify one molecular mechanism by which a highly prevalent tumour type can progresses to its malignant state.

Methods Summary

Mice, tumour initiation, and derivation of cell lines. *Kras*$^{LSL\text{-}G12D}$, *p53*^{flox}, *p53*$^{LSL\text{-}R270H}$, and *p53*$^{LSL\text{-}R172H}$ mice have been described[3,5,20]. Tumours were initiated by intratracheal infection of mice with a lentiviral vector expressing Cre-recombinase[10]. The MIT Institutional Animal Care and Use Committee approved all animal studies and procedures. Cell lines were created by enzymatic and mechanical dissociation of individual lung tumours and metastases harvested from mice 8-14 months after tumour initiation.

LM-PCR, Southern blotting, and gene expression analysis. LM-PCR was performed with forward primers specific for the lentiviral LTR. Southern blotting used Cre probe and standard methods. RNA was extracted using Trizol, analyzed for RNA integrity and prepared with Affymetrix GeneChip® WT Sense Target Labelling and Control Reagents kit, followed by hybridization to Affymetrix GeneChip® Mouse Exon 1.0 ST Arrays.

Protein and RNA analysis. Western blotting used standard methods and antibodies to Nkx2-1 (Epitomics, Inc), Hmga2 (BioCheck, Inc), and Hsp90 (BD Transduction Laboratories) as a loading control. Immunohistochemistry was performed on formalin-fixed, paraffin-embedded 4μm sections using the ABC Vectastain kit (Vector Laboratories) with antibodies described above. Sections were developed with DAB and counterstained with hematoxylin.

Gene expression and knockdown. Nkx2-1 was stably knocked-down with a pLKO-based lentiviral vector (OpenBiosystems/TRC). MSCV-Puro retroviral vectors were used for stable expression of Nkx2-1 and Nkx2-1* (created with 4 silent mutations using QuikChange® Lightning Site-Directed Mutagenesis (Stratagene). Hmga2 was stably knocked-down with an MSCV-Hygro retroviral vector.

Transplantation experiments. For intravenous transplantation 10^5 cells resuspended in 200μl PBS were injected in the lateral tail vein. For intrasplenic transplantation 10^5 cells resuspended in 50μl PBS. In all graphs each circle represents an individual mouse and the bar represents the mean. Statistical significance was determined using the Student's t-test.

Supplementary Information is linked to the online version of the paper at www.nature.com/nature.

Acknowledgements

The authors thank Alison Dooley, Nadya Dimitrova, Trudy Oliver, and Margaret Ebert for providing reagents; Manlin Luo (Biology/Koch Institute BioMicro Core) for array processing; Madhu Kumar for experimental assistance; Tracy Staton, David McFadden, Alice Shaw, and the entire Jacks laboratory for comments. M.M.W was a Merck Fellow of the Damon Runyon Cancer Research Foundation and is funded by a Genentech Postdoctoral Fellowship. R.G.W.V. is supported by a Fellowship from the Dutch Cancer Society KWF. E.L.S is supported by a training grant (T32-HL007627). D.M.F is a Leukemia and Lymphoma Postdoctoral Fellow. This work was supported by grants U54-CA126515 and U01-CA84306

from the National Institutes of Health, Howard Hughes Medical Institute, Ludwig Center for Molecular Oncology at MIT, and in part by the Cancer Center Support (core) grant P30-CA14051 from the National Cancer Institute. T.E.J. is the David H. Koch Professor of Biology and a Daniel K. Ludwig Scholar.

Author Contributions

M.M.W. and T.J. designed the study; M.M.W., T.L.D., C.K-K. performed experiments; R.G.W.V., C.A.W., D.D.H., S.H., and D.Y.C. conducted bioinformatic analyses; E.L.S. and R.T.B. provided pathology assistance; S.Y. and D.C. provided technical assistance; M.J.D. provided reagents; D.M.F. and M.M. gave conceptual advice; M.M.W and T.J wrote the paper with comments from all authors.

The authors declare no competing financial interests.

Correspondence and requests for materials should be addressed to T.J. (e-mail: tjacks@mit.edu)

Figure 1. A lentiviral-vector induced mouse model of lung adenocarcinoma identifies gene expression alterations during tumour progression. a, Infection of *Kras*$^{LSL\text{-}G12D/+}$;*p53*$^{flox/flox}$ mice with Cre-expressing lentiviral vectors initiates lung adenocarcinoma. **b,** Linker-mediated PCR cloning of the lentiviral integration site in metastases (Met) allows specific PCR amplification of that lentiviral-integration (lower band) to identify which primary tumour gave rise to the metastases. Top band is a control product. **c,** Southern blot for the integrated lentiviral genome on cell lines. **d,** Representative images of livers after intrasplenic transplantation of T_{nonMet} or T_{Met} cells. Scale bar = 0.5cm. **e,** Quantification of liver nodules after intrasplenic injection of two T_{nonMet} and T_{Met} cell lines. **f,** Gene expression alterations (log_2) between T_{nonMet} and T_{Met}/Met samples.

Figure 2. Reduced Nkx2-1 in advanced lung adenocarcinoma correlates with a less differentiated state. a, Cross-species analysis of human lung adenocarcinoma patient outcome (likelihood ratio with the sign from correlation value) versus differential gene expression in murine T_{nonMet} cells. **b,** Nkx2-1 protein is absent from T_{Met} and Met-derived cell lines. **c-d,** Nkx2-1 expression is high in well differentiated adenomas and early murine adenocarcinoma (top) but is downregulated in moderately to poorly differentiated advanced carcinomas (bottom). Scale bar = 50μm. Upper inlay Nkx2-1 staining. Lower inlay H+E staining. **e,** Quantification of Nkx2-1 expression in murine lung tumours relative to tumour grade from most differentiated (atypical adenomous hyperplasia (AAH)) to least differentiated (Poor)). **f,** Relative *NKX2-1* expression (log_2) in human lung adenocarcinomas correlates with a T_{nonMet} signature ($r^2 = 0.36$). The T_{nonMet} signature and an ES cell signature anti-correlate ($r^2 = -0.44$). Each vertical bar represents a lung adenocarcinoma sample. Scale bar indicates the signature score.

Figure 3. Nkx2-1 controls lung adenocarcinoma differentiation and restricts metastatic ability. a, Nkx2-1 protein reexpression in T_{Met} cells. **b,** Nkx2-1 reexpression reduces lung nodule formation after intravenous transplantation. $p < 0.002$. **c,** Quantification of Nkx2-1 in lung nodules after T_{Met} or T_{Met}-*Nkx2-1* transplantation. n=3/group. **d,** Association of Nkx2-1 expression with differentiation state in tumours after T_{Met} or T_{Met}-*Nkx2-1* transplantation. Fisher's exact test on the association of differentiation state with Nkx2-1 $p < 0.002$. **e,** Nkx2-1 reexpression reduces anchorage-independent growth of T_{Met} cells. Representative images and colony number (mean +/- SD of quadruplicate

wells, p < 0.0001). **f,** Nkx2-1 knockdown increases liver nodules after intrasplenic and lung nodules after intravenous transplantation of T_{nonMet} cells. Representative of 7 mice/group. **g,** *shNkx2-1* enhanced anchorage-independent growth of T_{nonMet} cells. Representative images and colony number (mean +/- SD of triplicate wells, p < 0.0001). **h,** Restoration of Nkx2-1 expression with an shRNA-insensitive *Nkx2-1* (*Nkx2-1**) in T_{nonMet}-*shNkx2-1* cells reverts the enhanced lung nodule formation after intravenous transplantation. Mean +/- SD, n=3/group. **i.** Induction of tumours in $Kras^{LSL\text{-}G12D/+}$;$p53^{flox/flox}$ mice with Nkx2-1/Cre lentivirus reduces the development of advanced tumours (grades 3&4). Numbers indicate percent of tumours in each group.

Figure 4. Nkx2-1 regulates the expression of Hmga2 in advanced lung adenocarcinoma. a, Nkx2-1 knockdown allows Hmga2 upregulation in T_{nonMet} cells. **b-c,** Hmga2 and Nkx2-1 are reciprocally expressed in $Kras^{G12D/+}$;$p53^{\Delta/\Delta}$ murine lung adenocarcinomas. Scale bar = 50μm. Inlaid images show cellular features and protein localization. Fisher's exact test, p-value < 10^{-11}. **d,** Early $Kras^{G12D/+}$;$p53^{\Delta/\Delta}$ tumours are Nkx2-1^{pos}Hmga2^{neg}. **e,** $Kras^{G12D}$-only tumours are Nkx2-1^{pos}Hmga2^{neg}. **f,** Expression of NKX2-1 and HMGA2 in human lung adenocarcinomas distributed by differentiation state. Large numbers are percentages. Small numbers are absolute number. **g,** Hmga2 knockdown reduces the tumourigenic potential of T_{nonMet}-*shNkx2-1* cells after intravenous transplantation. Control samples include the parental T_{nonMet}-*shNkx2-1* cells (grey circle) and cells infected by a control retrovirus (black circles). p < 0.003. **h,** *shHmga2* reduces anchorage-independent growth of a metastasis-derived cell line (Met). Representative images and colony number (mean +/- SD of

quadruplicate wells, $p < 0.0001$). **i,** *shHmga2* reduces the tumour-seeding potential of a Met cell line after intravenous transplantation. $p < 0.0001$.

1. Rodenhuis, S.*, et al.* Incidence and possible clinical significance of K-ras oncogene activation in adenocarcinoma of the human lung. *Cancer Res* **48**, 5738-5741 (1988).
2. Takahashi, T.*, et al.* p53: a frequent target for genetic abnormalities in lung cancer. *Science* **246**, 491-494 (1989).
3. Jonkers, J.*, et al.* Synergistic tumor suppressor activity of BRCA2 and p53 in a conditional mouse model for breast cancer. *Nat Genet* **29**, 418-425 (2001).
4. Jackson, E.L.*, et al.* The differential effects of mutant p53 alleles on advanced murine lung cancer. *Cancer Res* **65**, 10280-10288 (2005).
5. Jackson, E.L.*, et al.* Analysis of lung tumor initiation and progression using conditional expression of oncogenic K-ras. *Genes Dev* **15**, 3243-3248 (2001).
6. Weir, B.A.*, et al.* Characterizing the cancer genome in lung adenocarcinoma. *Nature* **450**, 893-898 (2007).
7. Tanaka, H.*, et al.* Lineage-specific dependency of lung adenocarcinomas on the lung development regulator TTF-1. *Cancer Res* **67**, 6007-6011 (2007).
8. Kendall, J.*, et al.* Oncogenic cooperation and coamplification of developmental transcription factor genes in lung cancer. *Proc Natl Acad Sci U S A* **104**, 16663-16668 (2007).
9. Kwei, K.A.*, et al.* Genomic profiling identifies TITF1 as a lineage-specific oncogene amplified in lung cancer. *Oncogene* **27**, 3635-3640 (2008).
10. DuPage, M., Dooley, A.L. & Jacks, T. Conditional mouse lung cancer models using adenoviral or lentiviral delivery of Cre recombinase. *Nat Protoc* **4**, 1064-1072 (2009).
11. Monti, S., Tamayo, P., Mesirov, J. & Golub, T. Consensus Clustering: A Resampling-Based Method for Class Discovery and Visualization of Gene Expression Microarray Data. *Machine Learning* **52**, 91-118 (2003).
12. Shedden, K.*, et al.* Gene expression-based survival prediction in lung adenocarcinoma: a multi-site, blinded validation study. *Nat Med* **14**, 822-827 (2008).
13. Nguyen, D.X.*, et al.* WNT/TCF signaling through LEF1 and HOXB9 mediates lung adenocarcinoma metastasis. *Cell* **138**, 51-62 (2009).
14. Kimura, S.*, et al.* The T/ebp null mouse: thyroid-specific enhancer-binding protein is essential for the organogenesis of the thyroid, lung, ventral forebrain, and pituitary. *Genes Dev* **10**, 60-69 (1996).
15. Krude, H.*, et al.* Choreoathetosis, hypothyroidism, and pulmonary alterations due to human NKX2-1 haploinsufficiency. *J Clin Invest* **109**, 475-480 (2002).
16. Maeda, Y., Dave, V. & Whitsett, J.A. Transcriptional control of lung morphogenesis. *Physiol Rev* **87**, 219-244 (2007).
17. Barletta, J.A.*, et al.* Clinical Significance of TTF-1 Protein Expression and TTF-1 Gene Amplification in Lung Adenocarcinoma. *J Cell Mol Med* (2008).
18. Berghmans, T.*, et al.* Thyroid transcription factor 1--a new prognostic factor in lung cancer: a meta-analysis. *Ann Oncol* **17**, 1673-1676 (2006).

19. Perner, S.*, et al.* TTF1 expression in non-small cell lung carcinoma: association with TTF1 gene amplification and improved survival. *J Pathol* **217**, 65-72 (2009).
20. Olive, K.P.*, et al.* Mutant p53 gain of function in two mouse models of Li-Fraumeni syndrome. *Cell* **119**, 847-860 (2004).
21. Ben-Porath, I.*, et al.* An embryonic stem cell-like gene expression signature in poorly differentiated aggressive human tumors. *Nat Genet* **40**, 499-507 (2008).
22. Nishino, J., Kim, I., Chada, K. & Morrison, S.J. Hmga2 promotes neural stem cell self-renewal in young but not old mice by reducing p16Ink4a and p19Arf Expression. *Cell* **135**, 227-239 (2008).
23. Yu, F.*, et al.* let-7 regulates self renewal and tumorigenicity of breast cancer cells. *Cell* **131**, 1109-1123 (2007).
24. Li, O., Vasudevan, D., Davey, C.A. & Droge, P. High-level expression of DNA architectural factor HMGA2 and its association with nucleosomes in human embryonic stem cells. *Genesis* **44**, 523-529 (2006).
25. Rommel, B.*, et al.* HMGI-C, a member of the high mobility group family of proteins, is expressed in hematopoietic stem cells and in leukemic cells. *Leuk Lymphoma* **26**, 603-607 (1997).
26. Fusco, A. & Fedele, M. Roles of HMGA proteins in cancer. *Nat Rev Cancer* **7**, 899-910 (2007).
27. Meyer, B.*, et al.* HMGA2 overexpression in non-small cell lung cancer. *Mol Carcinog* **46**, 503-511 (2007).
28. Hristov, A.C.*, et al.* HMGA2 protein expression correlates with lymph node metastasis and increased tumor grade in pancreatic ductal adenocarcinoma. *Mod Pathol* **22**, 43-49 (2009).
29. Rogalla, P.*, et al.* Expression of HMGI-C, a member of the high mobility group protein family, in a subset of breast cancers: relationship to histologic grade. *Mol Carcinog* **19**, 153-156 (1997).
30. Lee, Y.S. & Dutta, A. The tumor suppressor microRNA let-7 represses the HMGA2 oncogene. *Genes Dev* **21**, 1025-1030 (2007).

Jacks_Figure1

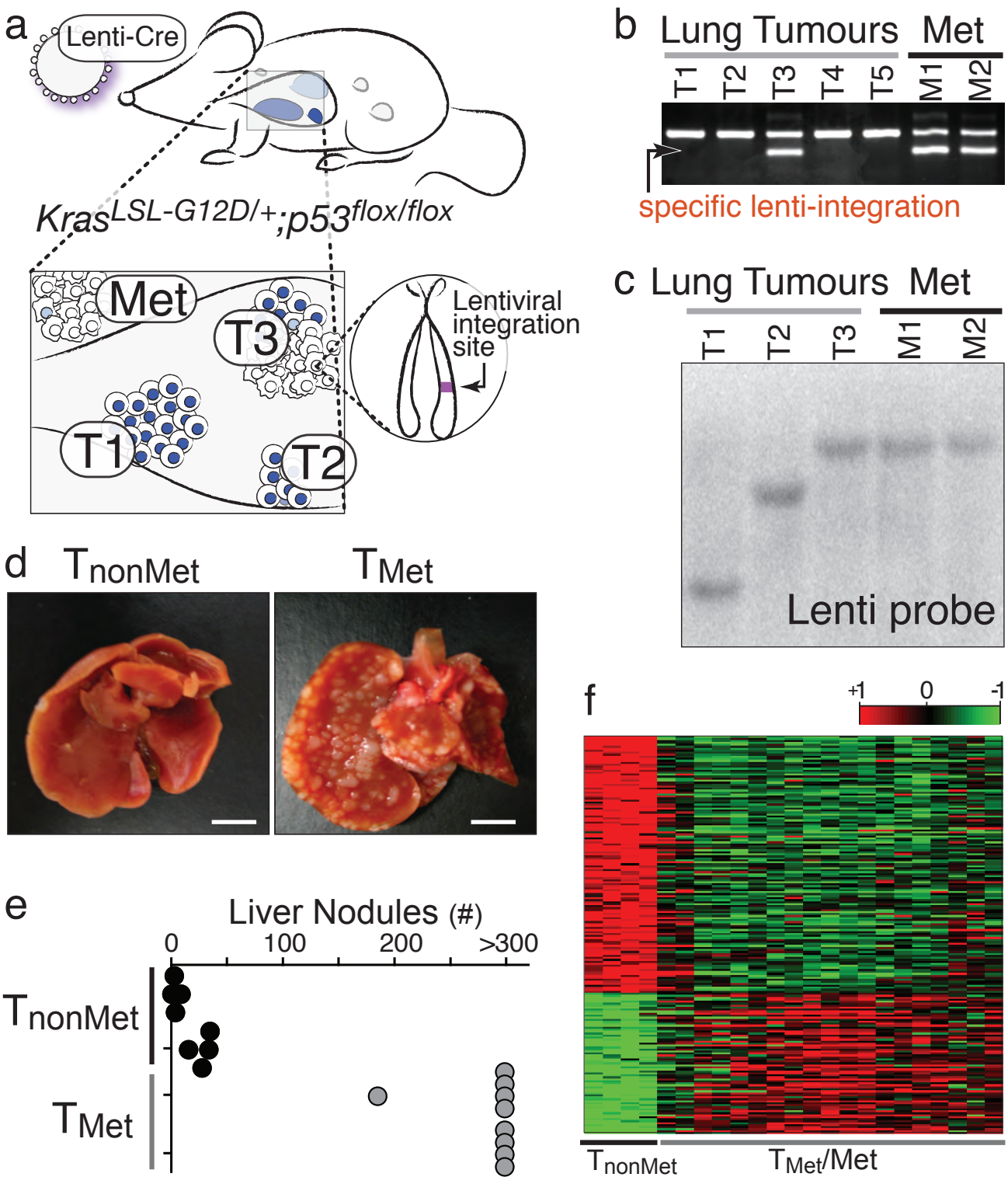

Jacks_Figure2

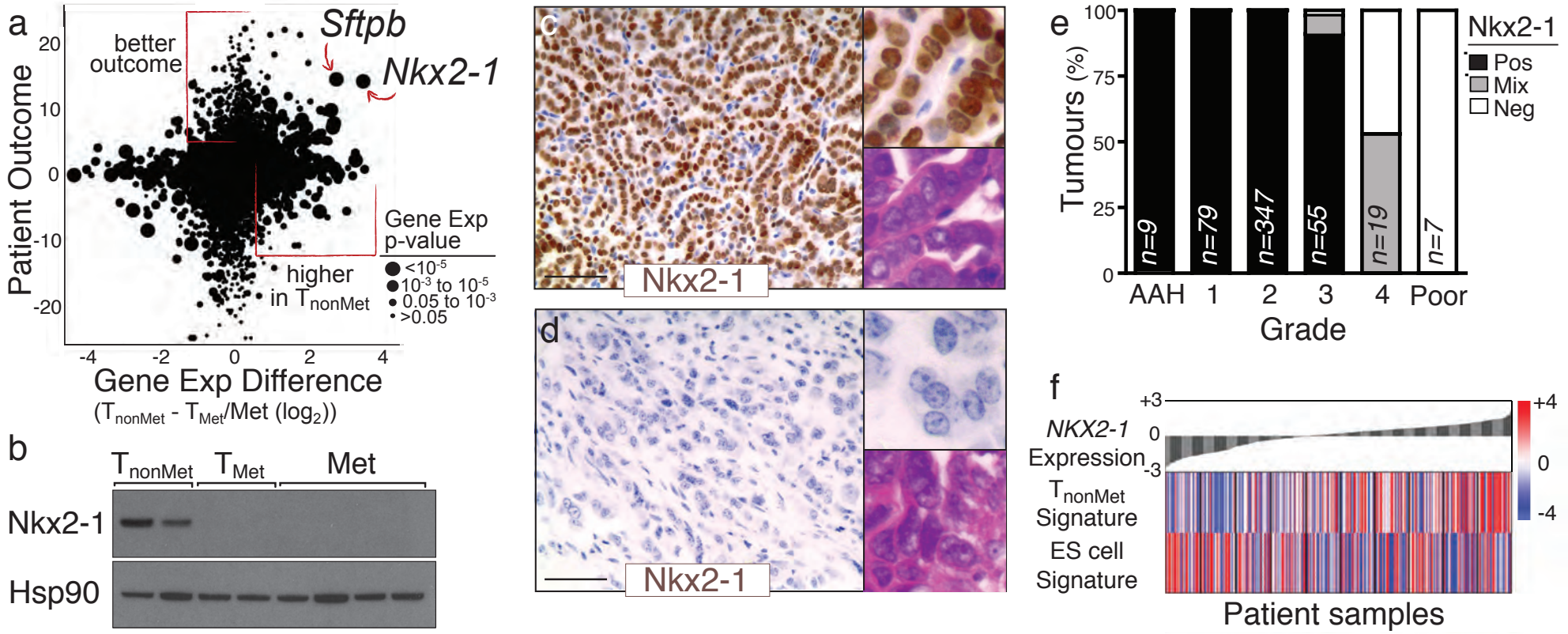

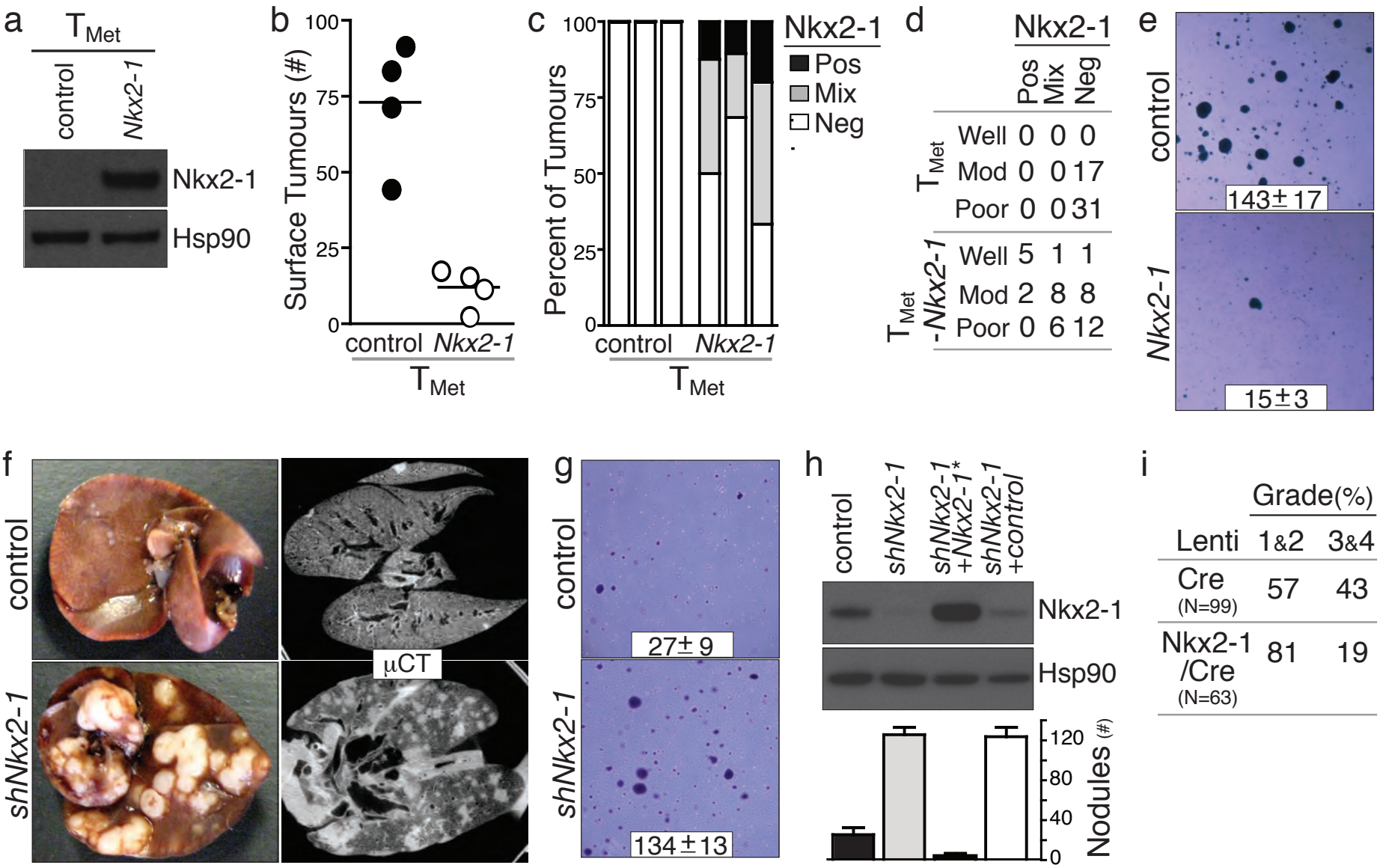
a
T Met
control
Nkx2-1
Nkx2-1
Hsp90
b
Surface Tumours (#)
100
75
50
25
0
control
Nkx2-1
T Met
c
Percent of Tumours
100
75
50
25
0
control
Nkx2-1
T Met
Nkx2-1
Pos
Mix
Neg
d
Nkx2-1
Pos Mix Neg
T Met
Well 0 0 0
Mod 0 0 17
Poor 0 0 31
T Met -Nkx2-1
Well 5 1 1
Mod 2 8 8
Poor 0 6 12
e
control
143±17
Nkx2-1
15±3
f
control
shNkx2-1
µCT
g
control
27±9
shNkx2-1
134±13
h
control
shNkx2-1
shNkx2-1 +Nkx2-1*
shNkx2-1 +control
Nkx2-1
Hsp90
120
80
40
0
Nodules (#)
i
Grade(%)
Lenti 1&2 3&4
Cre (N=99) 57 43
Nkx2-1 /Cre (N=63) 81 19

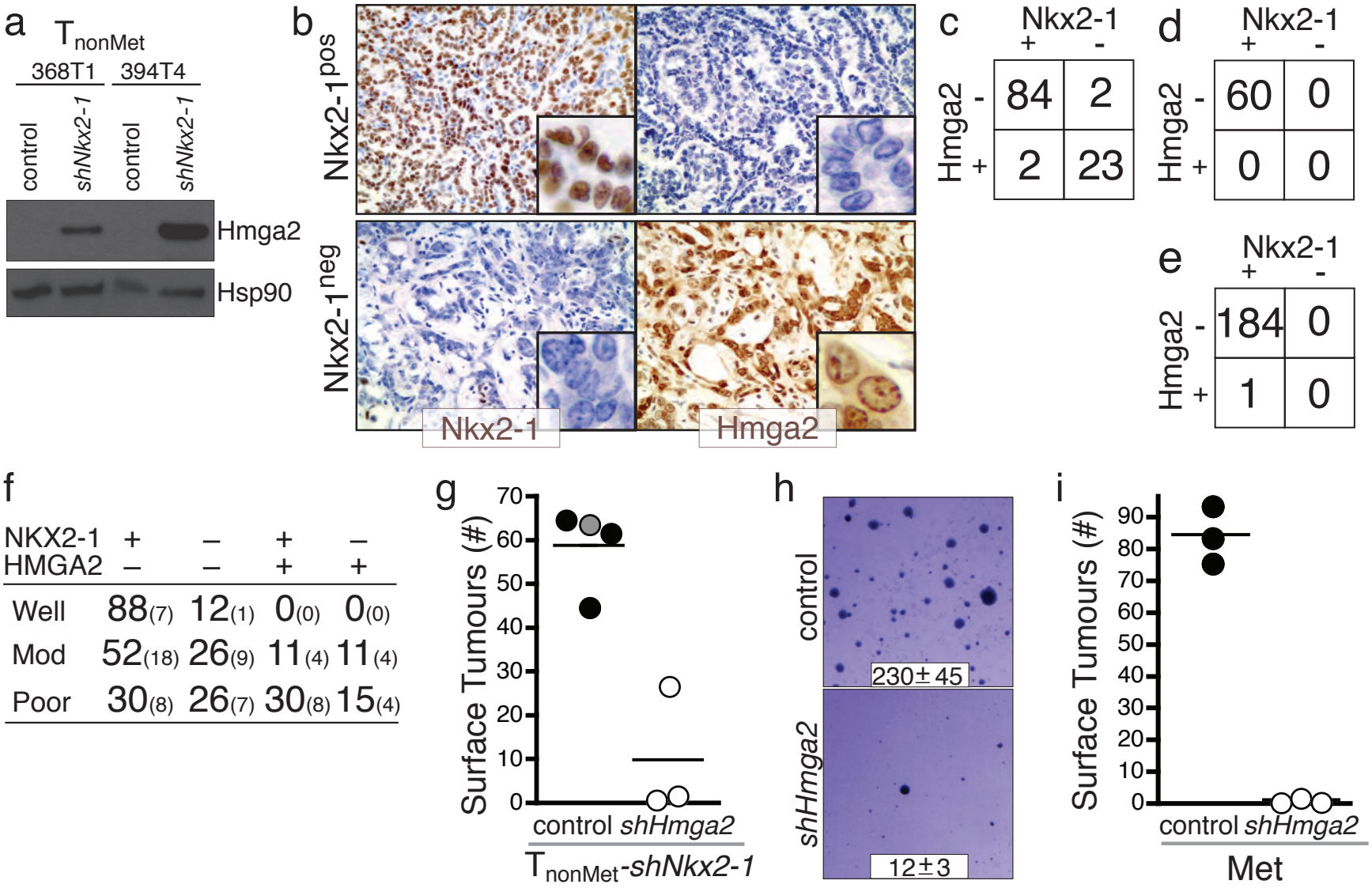
a
T nonMet
368T1
394T4
control
shNkx2-1
control
shNkx2-1
Hmga2
Hsp90
b
Nkx2-1pos
Nkx2-1neg
Nkx2-1
Hmga2
c
Nkx2-1
+
-
Hmga2
-
+
84
2
2
23
d
Nkx2-1
+
-
Hmga2
-
+
60
0
0
0
e
Nkx2-1
+
-
Hmga2
-
+
184
0
1
0
f
NKX2-1 + – + –
HMGA2 – – + +
Well 88(7) 12(1) 0(0) 0(0)
Mod 52(18) 26(9) 11(4) 11(4)
Poor 30(8) 26(7) 30(8) 15(4)
g
Surface Tumours (#)
70
60
50
40
30
20
10
0
control shHmga2
TnonMet-shNkx2-1
h
control
shHmga2
230±45
12±3
i
Surface Tumours (#)
90
80
70
60
50
40
30
20
10
0
control shHmga2
Met